

# An enhanced particle filtering method for GMTI radar tracking

Miao Yu<sup>+</sup>, Cunjia Liu<sup>+</sup>, Baibing Li<sup>\*</sup> and Wen-Hua Chen<sup>+</sup>

**Abstract**—This paper investigates the problem of ground vehicle tracking with a Ground Moving Target Indicator (GMTI) radar. In practice, the movement of ground vehicles may involve several different manoeuvring types (acceleration, deceleration, standstill, etc.). Consequently, the GMTI radar may lose measurements when the radial velocity of the ground vehicle is below a threshold, i.e. falling into the Doppler blind region. In this paper, to incorporate the information gathered from normal measurements and knowledge on the Doppler blindness constraint, we develop an enhanced particle filtering method for which the importance distributions are inspired by a recent noise related doppler blind (NRDB) filtering algorithm for GMTI tracking. Specifically, when constructing the importance distributions, the proposed particle filter takes the advantages of the efficient NRDB algorithm by applying the extended Kalman filter and its generalization for interval-censored measurements. In addition, the linearization and Gaussian approximations in the NRDB algorithm are corrected by the weighting process of the developed filtering method to achieve a more accurate GMTI tracking performance. The simulation results show that the proposed method substantially outperforms the existing methods for the GMTI tracking problem.

**Index Terms**—Particle filtering, GMTI, Target tracking, Doppler blind region, generalized EKF.

## I. INTRODUCTION

In this paper, we consider the problem of ground vehicle tracking using a Ground Moving Target Indicator (GMTI) radar which discriminates a moving target against the static background based on the Doppler effect [1]. GMTI radar is well suited for detecting targets moving on ground due to its wide-area, all-weather, day/night, and real-time capabilities [2]. Therefore, the GMTI-based tracking has received a wide range of applications in continuously tracking of vehicles to support the surveillance in different environments (e.g. battlefield and urban).

Due to its practical importance, there have been a number of methods developed in recent years to address various research issues associated with GMTI tracking. Kirubarajan et al. in [3] proposed a variable structure interacting multiple model (VS-IMM) algorithm for GMTI tracking, considering there may be more than one state model to describe the target object's movement and the number of state models may change as well. In order to overcome the nonlinearity in the measurement model of the GMTI radar and the non-Gaussian posterior distribution of the state vector, a particle filtering approach was proposed in [4] and the simulation results showed an improved performance with reduced root-mean-square-error (RMSE) than [3]. In addition, a new approach was proposed in [5] to improve on the

This work was supported by the Engineering and Physical Sciences Research Council (EPSRC) Grant number EP/J011525. Dr Miao Yu's involvement was supported by the EPSRC Grant number EP/K014307/1 and the MOD University Defence Research Collaboration in Signal Processing.

<sup>+</sup> Miao Yu, Cunjia Liu, and Wen-Hua Chen are with Department of Aeronautical and Automotive Engineering, Loughborough University, UK, LE11 3TU (e-mail: {m.yu,c.liu5,w.chen}@lboro.ac.uk).

<sup>\*</sup> Baibing Li is with the School of Business and Economics, Loughborough University, Loughborough LE11 3TU, UK, e-mail: b.li2@lboro.ac.uk.

performance of [4] in which the traditional particle filter was replaced with a more advanced unscented particle filter developed in [6].

The major limitation of the methods in [3], [4] and [5] is that the GMTI measurements were assumed to be recorded at every time step in these studies, which is not the case in the real-world problems. In practice, no GMTI measurements are received if the magnitude of a target object's radial velocity drops below the minimum detectable velocity.

In order to address this GMTI tracking problem, the researchers in [7] incorporated a separate stop model into the VS-IMM framework as a complement to the existing manoeuvring models. The incorporation of the stop model in the VS-IMM framework improves the tracking performance when no measurements are recorded due to vehicle stopping. On the other hand, there are some other studies such as [2], [8] and [9] that applied Gaussian mixture tracking algorithms by propagating the Gaussian mixture approximation to the conditional distribution of the target state. In addition, a suitable state-dependent detection probability was introduced, which helps to determine the conditional distribution of the target state when no measurements are recorded. To solve the problem that negative weights may possibly arise in the Gaussian mixture approximation, an extra approximation stage was introduced in [10] to replace the resulting negative Gaussian mixture with one having strictly positive mixture weights, and thus improving on algorithmic stability. The algorithm in [11] applied the particle filtering method and treated each non-detection case as evidence. The corresponding likelihood function of the non-detection evidence was formulated and incorporated into the particle filtering procedure to update the target state probability distribution when no measurements are recorded.

Recently, Clark et al. [12] have developed a new Gaussian Mixture Model (GMM) based noise related doppler blind (NRDB) filtering algorithm for GMTI tracking in which a GMM is used to approximate the posterior probability distribution of the state vector. This algorithm was carefully designed so that the Doppler blindness constraint of the GMTI radar can be efficiently dealt with under the Gaussian distribution assumption. The simulation results in [12] showed that this new approach outperformed some existing methods (such as [8]), especially when dealing with the scenario of no measurement. However, to ensure that the filter in [12] retains an analytically tractable form and to process signals efficiently, the following approximations have been made at each time step in this algorithm:

- *Approximation A.* A standard mixture reduction technique (see, e.g. [13]) is used to avoid the exponential growth of the number of the Gaussian mixture components;
- *Approximation B.* The posterior probability distribution of the state vector for each mode is approximated by a Gaussian distribution;
- *Approximation C.* The measurement equation associated with the GMTI radar is linearized based on the first-order Taylor expansion, and a Gaussian distribution assumption is made when dealing with the Doppler blindness constraint.

While *Approximation A* is the most commonly used approach to ensure the number of components is manageable in practice, *Approximation B* and *Approximation C* are adopted in [12] to form a generalized Extended Kalman filter (EKF) for the situation where a certain measurement is an interval-censored value, i.e. it falls into an

known interval (the Doppler blind region). More specifically, when the radial velocity of the target is within the Doppler blind region, Clark et al. [12] have made use of the results in [14] to compute conditional mathematical expectations and covariance matrices so that knowledge on the Doppler blindness constraint can be efficiently utilized to update the state estimate.

The aim of this paper is to address the limitations of the algorithm in [12] and remove *Approximations A-C* as much as possible. Because GMTI tracking is a nonlinear, non-Gaussian filtering problem, we will use a particle-filtering approach, rather than the GMM-based algorithm with EKF-like filtering in [12], to estimate the state vector.

First, we will use the resampling method developed in [15] to replace the mixture reduction technique adopted in *Approximation A* to ensure that the approximation errors are kept at a minimum level. In addition, we note that by applying the EKF and its generalized version, the GMM-based NRDB algorithm in [12] works very well in many scenarios. A distinguished feature of the method proposed in this paper is to fully take the advantages of the NRDB algorithm by treating the EKF and its generalized version as the importance distributions to generate particles in the proposed particle filter. The errors caused by the linearization and Gaussian approximations associated with the importance distributions (i.e. *Approximations B & C* outlined above) are then corrected in the later stage of the particle filter via a suitable weighting process.

This paper is divided into the following sections: Section II considers problem formulation of GMTI tracking and briefly introduces the Bayesian inference framework developed in [15]. The details of the proposed novel particle filtering algorithm for GMTI tracking are provided in Section III. A simulation study is given in Section IV that evaluates the numerical performance of the proposed method and compares its performance with other state-of-the-art methods. Finally, we conclude this paper with some concluding remarks in Section V.

## II. PROBLEM FORMULATION AND BAYESIAN FILTERING

### A. State and measurement models

In a standard tracking problem, the system model includes a state equation of the target object and a measurement model for the sensor observations. The state equation is used to describe the dynamics of the movement of the target vehicle and the measurements provide the information for state filtering. The movement of the ground target vehicle may involve several different manoeuvring types (acceleration, deceleration, standstill, etc.) and its dynamics are usually described using a Markov jump multiple model:

$$\mathbf{x}_t = \mathbf{F}(m_t)\mathbf{x}_{t-1} + \mathbf{w}_{t-1}(m_t) \quad (1)$$

where  $\mathbf{x}_t = [x_t, y_t, \dot{x}_t, \dot{y}_t]$  is the state vector consisting of the positions  $(x_t, y_t)$  and velocities  $(\dot{x}_t, \dot{y}_t)$  in  $x$  and  $y$  directions (here we assume that the vehicle moves on ground with  $z_t \equiv 0$  and  $\dot{z}_t \equiv 0$ ). Note that more than one movement mode are normally involved in the tracking problem with  $m_t \in \mathcal{M}$ , where  $\mathcal{M}$  is the set of mode indexes. The transitions among different modes are described by the transition probabilities. In this paper, we consider a Markov-jump system in [16] where the transition probability  $p(m_t = i | m_{t-1} = j)$  from mode  $j$  to  $i$  is assumed to be constant. In addition,  $\mathbf{F}(m_t)$  and  $\mathbf{w}_{t-1}(m_t)$  represent the state transition matrix and process noise which could depend on a particular movement mode  $m_t$ .

The standard GMTI radar measures the range, azimuth angle and range rate (denoted as  $y_r, y_\theta$  and  $y_{\dot{r}}$  at time step  $t$ , respectively) of the ground vehicle relative to the position of the GMTI radar. Following [12], we assume that these measurements are noise-corrupted from actual values such that

$$\mathbf{y}_t = \begin{bmatrix} y_r \\ y_\theta \\ y_{\dot{r}} \end{bmatrix} = h(\mathbf{x}_t) + \mathbf{n}_t = \begin{bmatrix} r_t \\ \theta_t \\ \dot{r}_t \end{bmatrix} + \begin{bmatrix} n_{r_t} \\ n_{\theta_t} \\ n_{\dot{r}_t} \end{bmatrix} \quad (2)$$

and

$$h(\mathbf{x}_t) = \begin{bmatrix} \sqrt{(x_t - x_{o,t})^2 + (y_t - y_{o,t})^2 + (z_t - z_{o,t})^2} \\ \arctan2(y_t - y_{o,t}, x_t - x_{o,t}) \\ \frac{(x_t - x_{o,t})(\dot{x}_t - \dot{x}_{o,t}) + (y_t - y_{o,t})(\dot{y}_t - \dot{y}_{o,t}) + (z_t - z_{o,t})(\dot{z}_t - \dot{z}_{o,t})}{\sqrt{(x_t - x_{o,t})^2 + (y_t - y_{o,t})^2 + (z_t - z_{o,t})^2}} \end{bmatrix} \quad (3)$$

where  $\arctan2$  denotes the four quadrant inverse tangent function,  $(x_{o,t}, y_{o,t}, z_{o,t})$  and  $(\dot{x}_{o,t}, \dot{y}_{o,t}, \dot{z}_{o,t})$  represent the position and velocity of the observer (GMTI radar) at time  $t$  respectively,  $h(\mathbf{x}_t) = [r_t, \theta_t, \dot{r}_t]^T$  is the ideal measurement vector without the measurement noises and  $\mathbf{n}_t = [n_{r_t}, n_{\theta_t}, n_{\dot{r}_t}]^T$  represents the measurement noise vector which is assumed to be Gaussian with zero-mean vector and a diagonal covariance matrix  $\text{diag}\{\sigma_r^2, \sigma_\theta^2, \sigma_{\dot{r}}^2\}$ . To reduce the non-linearity of (2), we adopt the unbiased measurement transformation method (see, e.g., [17] and [18] for details) to convert the non-linear measurement components  $r_t$  and  $\theta_t$  into the Cartesian measurements.

To deal with the Doppler blindness region, let  $\kappa$  denote the minimum detectable velocity of the GMTI radar, and let  $v_t^r$  denote the radial velocity of the target that is defined to be the target's velocity projected along the range direction. According to the properties of GMTI radars, no measurements will be detected if the target radial velocity is within the Doppler blind region. In addition, even the target radial velocity  $v_t^r$  is outside the Doppler blind region, the target is not always detected but with a detection probability  $P_D$  (see, e.g., [11]). The actual measurement  $\mathbf{z}_t$  takes the values in the set  $Z = \{R^3 \cup \emptyset\}$ , where  $\emptyset$  denotes a missing measurement, i.e.

$$\mathbf{z}_t = \begin{cases} \emptyset & |v_t^r| \leq \kappa \text{ or } |v_t^r| > \kappa \text{ with probability } 1 - P_D \\ \mathbf{y}_t & |v_t^r| > \kappa \text{ with probability } P_D. \end{cases} \quad (4)$$

### B. Bayesian inference for recursive filtering

Let  $\mathbf{X}_t = \{\mathbf{x}_1, \dots, \mathbf{x}_t\}$  and  $\mathbf{Z}_t = \{\mathbf{z}_1, \dots, \mathbf{z}_t\}$  denote the sequences of the state vectors and measurement vectors up to time step  $t$ . With the state space model (1)-(4), Bayesian inference can be drawn to derive the posterior distribution  $p(\mathbf{X}_t, m_t | \mathbf{Z}_t)$  at each time step  $t$ , which in turn can be used to determine both the mode probability  $p(m_t | \mathbf{Z}_t)$  and the mode-conditioned probability  $p(\mathbf{X}_t | m_t, \mathbf{Z}_t)$ . In this subsection, we briefly summarise the general recursive Bayesian filtering for the formulated estimation problem; see [15] for a detailed description.

Given the measurement sequence  $\mathbf{Z}_t = \{\mathbf{z}_1, \dots, \mathbf{z}_t\}$ , the recursive Bayesian filtering obtains the probability distribution  $p(\mathbf{X}_t, m_t | \mathbf{Z}_t)$  at each time step  $t$  using the previous distribution  $p(\mathbf{X}_{t-1}, m_{t-1} | \mathbf{Z}_{t-1})$  at  $t-1$ . First, we note that given  $p(\mathbf{X}_{t-1}, m_{t-1} | \mathbf{Z}_{t-1})$ ,  $p(\mathbf{X}_{t-1}, m_t | \mathbf{Z}_{t-1})$  can be obtained by law of total probability (termed mode interaction in [15]):

$$p(\mathbf{X}_{t-1}, m_t | \mathbf{Z}_{t-1}) = \sum_{m_{t-1} \in \mathcal{M}} p(m_t | m_{t-1}) p(\mathbf{X}_{t-1}, m_{t-1} | \mathbf{Z}_{t-1}). \quad (5)$$

On the basis of the mode interaction in (5) and the state transition probability distribution  $p(\mathbf{x}_t | \mathbf{X}_{t-1}, m_t, \mathbf{Z}_{t-1})$  defined in (1), the predicted distribution  $p(\mathbf{X}_t, m_t | \mathbf{Z}_{t-1})$  can be obtained:

$$p(\mathbf{X}_t, m_t | \mathbf{Z}_{t-1}) = p(\mathbf{x}_t | \mathbf{X}_{t-1}, m_t, \mathbf{Z}_{t-1}) p(\mathbf{X}_{t-1}, m_t | \mathbf{Z}_{t-1}). \quad (6)$$

Finally, following the Bayesian theorem, the posterior distribution of the state vector can be derived from the predicted distribution by taking into account the current measurement  $\mathbf{z}_t$ :

$$p(\mathbf{X}_t, m_t | \mathbf{Z}_t) \propto p(\mathbf{z}_t | \mathbf{x}_t) p(\mathbf{X}_t, m_t | \mathbf{Z}_{t-1}), \quad (7)$$

where  $p(\mathbf{z}_t | \mathbf{x}_t)$  is the likelihood function that is the probability of  $\mathbf{z}_t$  conditional on the state vector  $\mathbf{x}_t$ . Its definitions are given by the corresponding measurement model, Eqs. (2)-(4).

Hence, following the general Bayesian statistical inference procedure, the distribution  $p(\mathbf{X}_{t-1}, m_{t-1} | \mathbf{Z}_{t-1})$  at time step  $t-1$  can be updated to form the posterior distribution  $p(\mathbf{X}_t, m_t | \mathbf{Z}_t)$  at time step  $t$ . Furthermore, the marginal distribution  $p(\mathbf{x}_t, m_t | \mathbf{Z}_t)$  can be obtained

from  $p(\mathbf{X}_t, m_t | \mathbf{Z}_t)$ , upon which the state and mode estimations at time instance  $t$  can be worked out.

### III. THE PROPOSED ALGORITHM

#### A. The general structure

Overall, the enhanced particle filtering algorithm developed in this paper is based on Eqs. (5)-(7), and the filtered state vector at each time step  $t$  is derived by the corresponding marginal posterior distribution  $p(\mathbf{x}_t, m_t | \mathbf{Z}_t)$ .

First, we focus on Eq. (7). When there is a measurement recorded at  $t$ ,  $p(\mathbf{z}_t | \mathbf{x}_t)$  in Eq. (7) is given by Eq. (2). However, when there is no measurement (i.e.  $\mathbf{z}_t = \emptyset$ ), the likelihood function  $p(\mathbf{z}_t = \emptyset | \mathbf{x}_t)$  is given by (according to Eq. (4)):

$$\begin{aligned} p(\mathbf{z}_t = \emptyset | \mathbf{x}_t) &= p(-\kappa \leq v_t^r \leq \kappa | \mathbf{x}_t) \\ &+ (1 - P_D) \cdot (1 - p(-\kappa \leq v_t^r \leq \kappa | \mathbf{x}_t)) \\ &= (1 - P_D) + P_D p(-\kappa \leq v_t^r \leq \kappa | \mathbf{x}_t). \end{aligned} \quad (8)$$

In general, there is no exact analytical solution for the posterior distribution  $p(\mathbf{X}_t, m_t | \mathbf{Z}_t)$  for state and mode estimation. Recently Clark et al. in [12] have proposed an efficient GMM-based NRDB algorithm to approximate  $p(\mathbf{X}_t, m_t | \mathbf{Z}_t)$  on the basis of *Approximations A-C* as outlined in the previous section.

In order to address the limitations of the algorithm in [12] and to obtain more accurate state estimation, a novel particle filtering approach is developed as follows.

It is well known that the quality and efficiency of any particle filters depend on the quality of the chosen importance distribution. Ideally, the importance distribution should be: (a) close to the posterior distribution of the state vector and the mode, i.e.  $p(\mathbf{X}_t, m_t | \mathbf{Z}_t)$ ; and (b) easy to sample from. The ‘standard’ choice of importance distribution is the state transition distribution  $p(\mathbf{x}_t | \mathbf{X}_{t-1}, m_t, \mathbf{Z}_{t-1})$  given in Eq. (1). The main drawback of such a choice is that it does not take into account the current measurement  $\mathbf{z}_t$  (see, e.g. [16]) which reveals the state information.

Essentially the new filter to be developed in this paper includes two key elements. First, the EKF and its generalization for interval-censored measurements in [12] are used to construct the importance distributions. In comparison with the ‘standard’ choice of importance distribution, i.e. the state transition distribution at each state mode, the sampling efficiency is improved for each mode of the multiple models where the information about the current measurement  $\mathbf{z}_t$  has been incorporated. Secondly, all the three approximations in the NRDB algorithm are addressed by taking the advantages of particle filtering. This includes: (a) the standard mixture reduction technique is avoided by the resampling method; and (b) the linearization and Gaussian approximations are corrected through the weighting process in the proposed particle filter.

Specifically, at time  $t-1$ , suppose that for each mode  $s \in \mathcal{M}$ ,  $N$  weighted particles are allocated to the corresponding mode-matched filter,  $\{\mathbf{X}_{t-1}^{s,k}, w_{t-1}^{s,k}; k = 1, \dots, N\}$ , which are used to approximate the joint distribution  $p(\mathbf{X}_{t-1}, m_{t-1} = s | \mathbf{Z}_{t-1})$  as:

$$p(\mathbf{X}_{t-1}, m_{t-1} = s | \mathbf{Z}_{t-1}) \approx \sum_{k=1}^N w_{t-1}^{s,k} \delta(\mathbf{X}_{t-1} - \mathbf{X}_{t-1}^{s,k}), \quad (9)$$

where  $\delta(\cdot)$  is a Dirac delta function.

From (5), the mode interaction is given by:

$$\begin{aligned} p(\mathbf{X}_{t-1}, m_t = r | \mathbf{Z}_{t-1}) \\ \approx \sum_{s \in \mathcal{M}} \sum_{k=1}^N p(m_t = r | m_{t-1} = s) w_{t-1}^{s,k} \delta(\mathbf{X}_{t-1} - \mathbf{X}_{t-1}^{s,k}). \end{aligned} \quad (10)$$

Assuming the number of the state modes to be  $M$ , from Eq. (10) we can see that  $N \times M$  particles are required to represent  $p(\mathbf{X}_{t-1}, m_t = r | \mathbf{Z}_{t-1})$ . The increasing number of particles from  $N$  to  $N \times M$  for probability representation at each time step will

make the number of particles grow in an exponential way as time  $t$  becomes large.

Blom and Bloem in [15] developed a resampling method to address this problem, where the particles are resampled from the above distribution, conditional on the model  $m_t$ :

$$\begin{aligned} p(\mathbf{X}_{t-1} | m_t = r, \mathbf{Z}_{t-1}) \\ \approx \sum_{s \in \mathcal{M}} \sum_{k=1}^N \frac{p(m_t = r | m_{t-1} = s) w_{t-1}^{s,k} \delta(\mathbf{X}_{t-1} - \mathbf{X}_{t-1}^{s,k})}{p(m_t = r | \mathbf{Z}_{t-1})}, \end{aligned} \quad (11)$$

such that  $N$  new particles  $\bar{\mathbf{X}}_{t-1}^{r,k} \sim p(\mathbf{X}_{t-1} | m_t = r, \mathbf{Z}_{t-1})$  ( $k = 1, \dots, N$ ) are generated for each mode  $r$ , where  $p(m_t = r | \mathbf{Z}_{t-1})$  is the distribution of  $m_t$  for given  $\mathbf{Z}_{t-1}$ .

Because  $N$  is usually taken as a large number, the error caused by the above resampling process is small. In contrast, the number of modes in the NRDB algorithm is usually small or medium, and hence the standard mixture reduction technique used in [12] may not be able to well approximate a multi-modal posterior distribution.

Eqs. (6), (7) and (11) can be applied to derive the posterior distribution. See [15] for details. As mentioned earlier, this posterior is analytically intractable and hence Monte Carlo methods are usually used and new particles need to be drawn. In the particle filtering, this step is undertaken using an importance distribution.

Specifically, for each mode  $r$ , importance sampling is used to estimate the desired posterior distribution. Now suppose that a new sample  $\mathbf{x}_t^{r,k}$  of the current state vector  $\mathbf{x}_t$  is drawn from the importance distribution  $q_r(\mathbf{x}_t | \bar{\mathbf{X}}_{t-1}^{r,k}, \mathbf{Z}_t)$ . The obtained new state vector samples for time step  $t$  and the corresponding  $\bar{\mathbf{X}}_{t-1}^{r,k}$  form the particles at time step  $t$ :  $\mathbf{X}_t^{r,k} = [\bar{\mathbf{X}}_{t-1}^{r,k}, \mathbf{x}_t^{r,k}]$  ( $k = 1, \dots, N$ ).  $\mathbf{X}_t^{r,k}$ , together with the corresponding weights  $w_t^{r,k}$ , are used to represent the posterior distribution at time step  $t$ :

$$p(\mathbf{X}_t, m_t = r | \mathbf{Z}_t) \approx \sum_{k=1}^N w_t^{r,k} \delta(\mathbf{X}_t - \mathbf{X}_t^{r,k}), \quad (12)$$

upon which the marginal distribution  $p(\mathbf{x}_t, m_t = r | \mathbf{Z}_t)$  for the current state vector can be obtained.

According to whether GMTI measurements are recorded or not, different importance distributions  $q_r(\mathbf{x}_t | \bar{\mathbf{X}}_{t-1}^{r,k}, \mathbf{Z}_t)$  will be used in the proposed method. This will be investigated in detail below.

#### B. Particle filtering with measurements recorded

When the measurement at time step  $t$  is recorded, we have  $\mathbf{z}_t = \mathbf{y}_t$  given by Eq. (2). The EKF is applied to construct the importance distribution for every  $\bar{\mathbf{X}}_{t-1}^{r,k}$ . As in [6], we assume that in the local region nearby the state vector  $\bar{\mathbf{x}}_{t-1}^{r,k}$ , the mode-conditioned distribution  $p(\mathbf{x}_{t-1} | m_t = r, \mathbf{Z}_{t-1})$  is approximated as a Gaussian distribution  $\mathcal{N}(\mathbf{x}_{t-1} | \hat{\mathbf{x}}_{t-1|t-1}^{r,k}, \mathbf{P}_{t-1|t-1}^{r,k})$  with mean  $\hat{\mathbf{x}}_{t-1|t-1}^{r,k}$  and covariance matrix  $\mathbf{P}_{t-1|t-1}^{r,k}$ . The EKF estimates the Gaussian approximation of  $p(\mathbf{x}_t | m_t = r, \mathbf{Z}_t)$  in a local region, which is taken as the importance distribution  $q_r(\mathbf{x}_t | \bar{\mathbf{X}}_{t-1}^{r,k}, \mathbf{Z}_t)$  for the new particle generation.

The EKF scheme follows the standard Kalman filtering procedure by approximating the nonlinear measurement model via its first-order Taylor expansion. It is divided into the following prediction and correction steps:

*Prediction:*

$$\hat{\mathbf{x}}_{t|t-1}^{r,k} = \mathbf{F}_t^r \hat{\mathbf{x}}_{t-1|t-1}^{r,k}, \quad (13)$$

$$\mathbf{P}_{t|t-1}^{r,k} = \mathbf{F}_t^r \mathbf{P}_{t-1|t-1}^{r,k} (\mathbf{F}_t^r)^T + \mathbf{Q}_t^r, \quad (14)$$

Correction:

$$\tilde{\mathbf{y}}_t^{r,k} = \mathbf{z}_t - h(\hat{\mathbf{x}}_{t|t-1}^{r,k}), \quad (15)$$

$$\mathbf{S}_t^{r,k} = \mathbf{H}_t^{r,k} \mathbf{P}_{t|t-1}^{r,k} (\mathbf{H}_t^{r,k})^T + \mathbf{R}_t, \quad (16)$$

$$\mathbf{K}_t^{r,k} = \mathbf{P}_{t|t-1}^{r,k} (\mathbf{H}_t^{r,k})^T (\mathbf{S}_t^{r,k})^{-1}, \quad (17)$$

$$\hat{\mathbf{x}}_{t|t}^{r,k} = \hat{\mathbf{x}}_{t|t-1}^{r,k} + \mathbf{K}_t^{r,k} \tilde{\mathbf{y}}_t^{r,k}, \quad (18)$$

$$\mathbf{P}_{t|t}^{r,k} = (\mathbf{I} - \mathbf{K}_t^{r,k} \mathbf{H}_t^{r,k}) \mathbf{P}_{t|t-1}^{r,k}, \quad (19)$$

where  $\hat{\mathbf{x}}_{t-1|t-1}^{r,k}$  and  $\mathbf{P}_{t-1|t-1}^{r,k}$  represent the initial mean and covariance matrix associated with the particle  $\bar{\mathbf{X}}_{t-1}^{r,k}$ .  $\mathbf{Q}_{t-1}^r$  and  $\mathbf{R}_t$  are the covariance matrices of the process noise  $\mathbf{w}_{t-1}(m_t)$  with  $m_t = r$  in (1) and the measurement noise  $\mathbf{n}_t$  in (2) respectively.  $\mathbf{F}_t^r$  is  $\mathbf{F}(m_t)$  evaluated at  $m_t = r$ .  $\mathbf{H}_t^{r,k}$  is the gradients of  $h(\mathbf{x}_t)$  evaluated at the point of  $\hat{\mathbf{x}}_{t|t-1}^{r,k}$ :

$$\mathbf{H}_t^{r,k} = \frac{\partial h(\mathbf{x}_t)}{\partial \mathbf{x}_t} \Big|_{\hat{\mathbf{x}}_{t|t-1}^{r,k}}. \quad (20)$$

The obtained Gaussian distribution  $\mathcal{N}(\mathbf{x}_t | \hat{\mathbf{x}}_{t|t}^{r,k}, \mathbf{P}_{t|t}^{r,k})$  is taken as the importance distribution  $q_r(\mathbf{x}_t | \bar{\mathbf{X}}_{t-1}^{r,k}, \mathbf{Z}_t)$  for generating new state particles. Clearly, the measurement information is incorporated for constructing  $\mathcal{N}(\mathbf{x}_t | \hat{\mathbf{x}}_{t|t}^{r,k}, \mathbf{P}_{t|t}^{r,k})$  so that the generated particles are more likely in the high measurement likelihood region.

It should be noted that Eq. (16) involves the inverse of a matrix for every particle  $\bar{\mathbf{X}}_{t-1}^{r,k}$ , and thus potentially it requires a substantial amount of computational time. In order to reduce the computation cost, we set every initial covariance  $\mathbf{P}_{t-1|t-1}^{r,k}$  ( $k = 1, \dots, N$ ) to be equal to a pre-set matrix  $\tau \text{diag}\{1, 1, \tau_0, \tau_0\}$  with  $\tau$  and  $\tau_0$  being two tuning parameters. In addition, the gradient of  $h(\mathbf{x}_t)$  is evaluated at a common value,  $\frac{1}{N} \sum_{k=1}^N \hat{\mathbf{x}}_{t|t-1}^{r,k}$ , which are in turn used to approximate  $\mathbf{H}_t^{r,k}$  for each  $k$ . In doing so, only one matrix inverse is needed for estimating the importance distribution for each particle.

### C. Particle filtering without measurements

When there is no measurement recorded at a time step  $t$ , i.e.  $\mathbf{z}_t = \emptyset$ , either the target radial velocity is within the Doppler blindness constraint region ( $|v_t^r| \leq \kappa$ ) or the target is not detected (with probability  $1 - P_D$ ). For each mode  $m_t = r$ , the mode-conditioned probability of the state vector  $\mathbf{x}_t$  follows:

$$\begin{aligned} p(\mathbf{x}_t | m_t = r, \mathbf{Z}_t) &\propto (1 - P_D) p(\mathbf{x}_t | m_t = r, \mathbf{Z}_{t-1}) \\ &+ P_D p(\mathbf{x}_t | m_t = r, \mathbf{Z}_{t-1}, |v_t^r| \leq \kappa) p(|v_t^r| \leq \kappa | m_t = r, \mathbf{Z}_{t-1}). \end{aligned} \quad (21)$$

Similar to the scenario that the measurements are recorded, we use a mixture of two Gaussian distributions to approximate the local distribution of  $p(\mathbf{x}_t | m_t = r, \mathbf{Z}_t)$ . This Gaussian mixture distribution is taken as the importance distribution for generating a new state particle. This will be discussed in detail below.

For the first term in (21), the probability  $p(\mathbf{x}_t | m_t = r, \mathbf{Z}_{t-1})$  represents the predicted distribution based on the previous measurements  $\mathbf{Z}_{t-1}$ . From the approximated initial Gaussian distribution  $\mathcal{N}(\mathbf{x}_{t-1} | \hat{\mathbf{x}}_{t-1|t-1}^{r,k}, \mathbf{P}_{t-1|t-1}^{r,k})$  nearby the particle  $\bar{\mathbf{x}}_{t-1}^{r,k}$  (as in the previous subsection), the predicted distribution can be approximated as a Gaussian distribution with the mean  $\hat{\mathbf{x}}_{t|t-1}^{r,k}$  and covariance  $\mathbf{P}_{t|t-1}^{r,k}$ . The recursive formulae are identical to the ones given previously.

We now turn to consider the second term of (21). Note that now the only information we know is that the target radial velocity  $v_t^r$  falls into a given interval, i.e.  $|v_t^r| \leq \kappa$ . This is termed interval-censored problem in the literature. To deal with this interval-censored problem, we follow [12] and use the results in [14] to work out the mathematical expectation and variance conditional on the interval-censored measurement  $v_t^r$  (see Appendix A for the detailed results) as follows.

First, we approximate the target radial velocity by the first-order Taylor expansion around the predicted state  $\hat{\mathbf{x}}_{t|t-1}^{r,k}$  as:

$$v_t^r(\mathbf{x}_t) = v_t^r(\hat{\mathbf{x}}_{t|t-1}^{r,k}) + \frac{\partial v_t^r(\mathbf{x}_t)}{\partial \mathbf{x}_t} \Big|_{\hat{\mathbf{x}}_{t|t-1}^{r,k}} (\mathbf{x}_t - \hat{\mathbf{x}}_{t|t-1}^{r,k}). \quad (22)$$

From (22), the conditional mean  $\hat{\mathbf{x}}_{t|t}^{r,k}$  and covariance  $\mathbf{P}_{t|t}^{r,k}$  of  $p(\mathbf{x}_t | m_t = r, \mathbf{Z}_{t-1}, |v_t^r| \leq \kappa)$  can be calculated using the formulae in Appendix A:

$$\hat{\mathbf{x}}_{t|t}^{r,k} = \hat{\mathbf{x}}_{t|t-1}^{r,k} + \mathbf{K}_t^{r,k} (m_A^{r,k} - v_t^r(\hat{\mathbf{x}}_{t|t-1}^{r,k})), \quad (23)$$

$$\mathbf{K}_t^{r,k} = \mathbf{P}_{t|t-1}^{r,k} (\mathbf{H}_t^{r,k})^T (\mathbf{H}_t^{r,k} \mathbf{P}_{t|t-1}^{r,k} (\mathbf{H}_t^{r,k})^T + \mathbf{V}_A^{r,k})^{-1}, \quad (24)$$

$$\mathbf{P}_{t|t}^{r,k} = \mathbf{P}_{t|t-1}^{r,k} - \mathbf{K}_t^{r,k} \mathbf{H}_t^{r,k} \mathbf{P}_{t|t-1}^{r,k} + \mathbf{K}_t^{r,k} \mathbf{V}_A^{r,k} (\mathbf{K}_t^{r,k})^T, \quad (25)$$

where  $\mathbf{H}_t^{r,k} = \frac{\partial v_t^r(\mathbf{x}_t)}{\partial \mathbf{x}_t} \Big|_{\hat{\mathbf{x}}_{t|t-1}^{r,k}}$  and

$$\begin{aligned} m_A^{r,k} &= (\gamma_t^{r,k})^{-1} (\bar{\sigma}^{r,k})^2 [\mathcal{N}(-\kappa | v_t^r(\hat{\mathbf{x}}_{t|t-1}^{r,k}), (\bar{\sigma}^{r,k})^2) \\ &\quad - \mathcal{N}(\kappa | v_t^r(\hat{\mathbf{x}}_{t|t-1}^{r,k}), (\bar{\sigma}^{r,k})^2)] + v_t^r(\hat{\mathbf{x}}_{t|t-1}^{r,k}), \end{aligned} \quad (26)$$

$$\begin{aligned} \mathbf{V}_A^{r,k} &= (\gamma_t^{r,k})^{-1} (\bar{\sigma}^{r,k})^2 [(-\kappa + v_t^r(\hat{\mathbf{x}}_{t|t-1}^{r,k})) \mathcal{N}(-\kappa | v_t^r(\hat{\mathbf{x}}_{t|t-1}^{r,k}), (\bar{\sigma}^{r,k})^2) \\ &\quad - (\kappa + v_t^r(\hat{\mathbf{x}}_{t|t-1}^{r,k})) \mathcal{N}(\kappa | v_t^r(\hat{\mathbf{x}}_{t|t-1}^{r,k}), (\bar{\sigma}^{r,k})^2)] \\ &\quad + ((v_t^r(\hat{\mathbf{x}}_{t|t-1}^{r,k}))^2 + (\bar{\sigma}^{r,k})^2) - (m_A^{r,k})^2, \end{aligned} \quad (27)$$

$$\bar{\sigma}^{r,k} = (\mathbf{H}_t^{r,k} \mathbf{P}_{t|t-1}^{r,k} (\mathbf{H}_t^{r,k})^T)^{1/2}. \quad (28)$$

This procedure is a generalization of the EKF to the problem of state estimation based on an interval-censored measurement. On the basis of this generalized EKF, the distribution  $p(\mathbf{x}_t | m_t = r, \mathbf{Z}_{t-1}, |v_t^r| \leq \kappa)$  can be approximated as  $N(\mathbf{x}_t | \hat{\mathbf{x}}_{t|t}^{r,k}, \mathbf{P}_{t|t}^{r,k})$ . In addition, based on Eq. (22), the probability that the measured range rate is within the Doppler blind zone, i.e.  $p(|v_t^r| \leq \kappa | m_t = r, \mathbf{Z}_{t-1})$ , is approximated by

$$\gamma_t^{r,k} = \int_{-\kappa}^{\kappa} \mathcal{N}(x | v_t^r(\hat{\mathbf{x}}_{t|t-1}^{r,k}), (\bar{\sigma}^{r,k})^2) dx. \quad (29)$$

Finally, on the basis of the above analysis, we choose the importance distribution for each particle  $\bar{\mathbf{X}}_{t-1}^{r,k}$  as:

$$\begin{aligned} q_r(\mathbf{x}_t | \bar{\mathbf{X}}_{t-1}^{r,k}, \mathbf{Z}_t) &\propto \\ &(1 - P_D) \mathcal{N}(\mathbf{x}_t | \hat{\mathbf{x}}_{t|t-1}^{r,k}, \mathbf{P}_{t|t-1}^{r,k}) + P_D \gamma_t^{r,k} \mathcal{N}(\mathbf{x}_t | \hat{\mathbf{x}}_{t|t}^{r,k}, \mathbf{P}_{t|t}^{r,k}). \end{aligned} \quad (30)$$

#### Remarks:

- (i) The above importance distribution is a Gaussian mixture distribution, and thus it is straightforward to draw particles from this distribution.
- (ii) It can be seen from the construction of the importance distribution Eq. (30) that, when no measurement is recorded, the relevant information is incorporated by taking into account the Doppler blindness constraint,  $|v_t^r| \leq \kappa$ . The constructed importance distribution is a local approximation of the desired distribution  $p(\mathbf{x}_t | m_t = r, \mathbf{Z}_t)$  so that the particles of  $p(\mathbf{x}_t | m_t = r, \mathbf{Z}_t)$  can be generated from the importance distribution.
- (iii) Similar to the scenario that the measurements are recorded, we set the initial covariance  $\mathbf{P}_{t-1|t-1}^{r,k}$  ( $k = 1, \dots, N$ ) to be equal and each  $\mathbf{H}_t^{r,k}$  is approximated by the first order gradient of the radial velocity evaluated at the averaged predicted means. In doing so, only one  $\bar{\sigma}^{r,k}$  and one  $\mathbf{K}_t^{r,k}$  are needed to calculate for all the particles, and hence the computational cost is reduced.

### D. Correcting the approximation errors

It can be seen from the previous subsections that several approximations were made when deriving the importance distributions. The

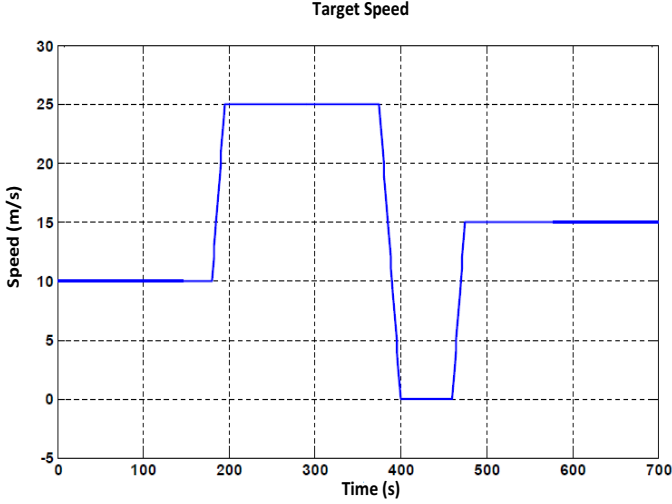


Fig. 1. The speed of the manoeuvring ground vehicle.

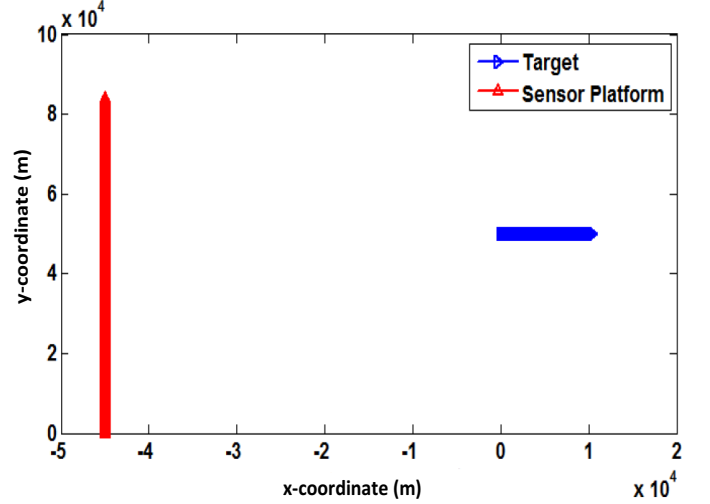


Fig. 2. The trajectories of the ground target and sensor platform.

corresponding approximation errors can be corrected in the proposed particle filtering algorithm through a weighting operation.

Suppose that we have drawn a new state vector particle  $\mathbf{x}_t^{r,k}$  from the importance distribution  $q_r(\mathbf{x}_t|\bar{\mathbf{X}}_{t-1}^{r,k}, \mathbf{Z}_t)$  and hence formed a new particle  $\mathbf{X}_t^{r,k} = [\bar{\mathbf{x}}_{t-1}^{r,k}, \mathbf{x}_t^{r,k}]$ . The corresponding weight for each new particle  $\mathbf{X}_t^{r,k}$  is given by the following ratio:

$$w_t^{r,k} \propto p(m_t = r|\mathbf{Z}_{t-1}) \frac{p(\mathbf{z}_t|\mathbf{x}_t^{r,k})p(\bar{\mathbf{x}}_{t-1}^{r,k}|\bar{\mathbf{X}}_{t-1}^{r,k}, m_t = r, \mathbf{Z}_t)}{q_r(\mathbf{x}_t^{r,k}|\bar{\mathbf{X}}_{t-1}^{r,k}, \mathbf{Z}_t)}. \quad (31)$$

Each particle  $\mathbf{X}_t^{r,k}$  is assigned a suitable weight  $w_t^{r,k}$ . This results in an estimate of the posterior distribution, Eq. (12). Two things are worth noting from (31):

(i) In some practical problems, the state transition probability distribution given by the state equation (1) is rank-deficient and  $p(\mathbf{x}_t^{r,k}|\bar{\mathbf{X}}_{t-1}^{r,k}, m_t = r, \mathbf{Z}_t)$  could not be calculated directly. We apply the QR decomposition to solve this problem (the details are presented in Appendix B).

(ii) We have used a novel importance distribution which is estimated from either the EKF or the generalized EKF to incorporate the GMTI measurement information, and therefore the weight in Eq. (31) is different from that used in [15]. In [15], the importance distribution is chosen as the system transition distribution  $p(\mathbf{x}_t|\bar{\mathbf{x}}_{t-1}, m_t = r)$  and hence  $w_t^{r,k} \propto p(m_t = r|\mathbf{Z}_{t-1})p(\mathbf{z}_t|\mathbf{x}_t^{r,k})$ .

#### IV. SIMULATION STUDY

In this section, we use a simulation study to evaluate the numerical performance of the developed filter.

A simulation study was carried out for a single target tracking scenario in which a GMTI sensor mounted on an airborne platform was employed to track the motion of a moving ground vehicle. The target moving eastbound started at a constant speed of 10 m/s and maintained for 180 s before it accelerated at a rate of 1 m/s<sup>2</sup> up to a speed of 25 m/s. After travelling at this constant speed for 180 s, the target started to decelerate for 25 s until it came to a standstill. The target remained stationary for 60 s, before accelerating again to a speed of 15 m/s. Target speed as a function of time is plotted in Figure 1. The same simulation scenario was also investigated in [12].

The sensor platform travelled northbound at a constant speed of 120 m/s and at an altitude of 10 km. The moving sensor platform took noisy measurements (including the 3-D range, azimuth angle and range rate) of the ground-moving target every 5s. The movements of the target and sensor platform are displayed in Figure 2.

#### A. The state and measurement models

Because the vehicle moved in several different manoeuvring styles, we applied a multiple models scheme to describe the movement of the target. Following [12], [19], we define a low-intensity nearly constant velocity (LINCVC) model, a high-intensity nearly constant velocity (HINCVC) model. In addition, a stop model based on the nearly constant position (NCP) model in [20] is used to model the scenario of vehicle stopping.

To better compare the proposed algorithm with the GMM-based NRDB algorithm in [12], we used the same way to discretise the continuous-time model of vehicle dynamics, and assumed the following general form of state equation for every model (see, e.g. [21], for other forms of the discretised state equation in the literature):

$$\mathbf{x}_t = \mathbf{F}(m_t)\mathbf{x}_{t-1} + \mathbf{G}(m_t)\mathbf{w}_{t-1}(m_t), \quad (32)$$

where  $m_t = \{1, 2, 3\}$  represents the model index:  $m_t = 1$  for the LINCVC model,  $m_t = 2$  for the HINCVC model and  $m_t = 3$  for the Stop mode. A Gaussian distribution is assumed for the  $2 \times 1$  noise vector  $\mathbf{w}_{t-1}(m_t)$  with zero means and mode related covariance matrix  $\text{diag}\{\sigma_x^2(m_t), \sigma_y^2(m_t)\}$  with: (a)  $\sigma_x^2(m_t) = \sigma_y^2(m_t) = 0.05^2(\text{m/s}^2)^2$  for  $m_t = 1$ ; (b)  $\sigma_x^2(m_t) = \sigma_y^2(m_t) = 0.5^2(\text{m/s}^2)^2$  for  $m_t = 2$ ; and (c)  $\sigma_x^2(m_t) = \sigma_y^2(m_t) = 0.005^2(\text{m/s}^2)^2$  for  $m_t = 3$ .

The state transition matrix  $\mathbf{F}(m_t)$  and constant matrix  $\mathbf{G}(m_t)$  for  $m_t = \{1, 2\}$  are defined as:

$$\mathbf{F}(m_t) = \begin{bmatrix} 1 & 0 & T & 0 \\ 0 & 1 & 0 & T \\ 0 & 0 & 1 & 0 \\ 0 & 0 & 0 & 1 \end{bmatrix}, \quad \mathbf{G}(m_t) = \begin{bmatrix} T^2/2 & 0 \\ 0 & T^2/2 \\ T & 0 \\ 0 & T \end{bmatrix}, \quad (33)$$

where  $T = 5\text{s}$  is the time interval between two consecutive samplings.

For the Stop model with  $m_t = 3$ ,  $\mathbf{F}(3)$  and  $\mathbf{G}(3)$  are defined as:

$$\mathbf{F}(3) = \begin{bmatrix} 1 & 0 & 0 & 0 \\ 0 & 1 & 0 & 0 \\ 0 & 0 & 0 & 0 \\ 0 & 0 & 0 & 0 \end{bmatrix}, \quad \mathbf{G}(3) = \begin{bmatrix} T & 0 \\ 0 & T \\ 0 & 0 \\ 0 & 0 \end{bmatrix}. \quad (34)$$

where the evolution of the position is modeled by adding non-zero process noise as in [20]. In addition, the velocity is forced to be zero as in [22] and [23].

The relevant model transition probabilities were calculated according to the method described in [7], and the resulting state mode

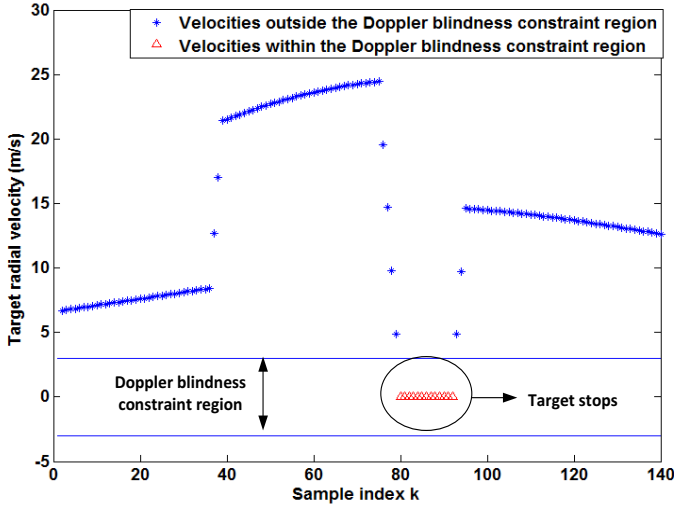


Fig. 3. The target radial velocities. When the vehicle stops (the target radial velocities are zero), no measurements are recorded.

transition matrix is given by:

$$\begin{pmatrix} 0.9500 & 0.0495 & 0.0005 \\ 0.2182 & 0.7273 & 0.0545 \\ 0.0008 & 0.0825 & 0.9167 \end{pmatrix}. \quad (35)$$

The measurement model, as discussed in Section II, includes two scenarios: measurements recorded and not recorded. As illustrated in Figure 3, when a measurement is recorded and the target's radial velocity is outside the Doppler blindness constraint region  $(-\kappa, +\kappa)$  (here we followed [12] and set  $\kappa$  to be 3 m/s), the corresponding likelihood function is Gaussian as given by (2). In the simulation study, we followed [12] and set the parameters of the measurement equation,  $\sigma_r$  and  $\sigma_\theta$ , as 20 m and 0.001 rad respectively. On the other hand, when no measurement is recorded, the measurement model is given by Eq.(8). Finally, throughout the simulation study, the two tuning parameters  $\tau$  and  $\tau_0$  were set as 1 and 0.1 respectively.

### B. Tracking performance analysis

Based on the state and measurement models, the proposed algorithm was applied for the tracking of the moving target in the set scenario and the corresponding tracking performance was evaluated. As in [12], we assumed the initial target state distribution followed a single Gaussian prior density obtained by the single-point (SP) track initialization algorithm ([24] and [25]) for the proposed approach and for the other algorithms used for comparison below.

The manoeuvring types of the moving target at different time points are shown in Figure 4 (a), and the estimated model probabilities using the proposed algorithm are given in Figure 4 (b). It can be seen that at the majority of time instances, the model that corresponded to the actual movement type had the largest probability. Hence, the manoeuvring characteristics of the moving target could be correctly reflected by the proposed algorithm in the simulation study.

Next, we analyse the tracking accuracy of the proposed method and draw a comparison with some other state-of-the-art approaches, including the multiple model version of the noise related Doppler blind mixture filter (NRDB-MM) [12] and the multiple model particle filtering (MMPF) approach. Here the multiple-model-based approaches were chosen for a fair comparison as our proposed approach considers multiple state models. In particular, the NRDB-MM algorithm in [12] was used as the benchmark algorithm for comparison purposes, whereas the MMPF approach is a widely used algorithm in the literature (see, e.g., [11], [4] and [26]). The parameter

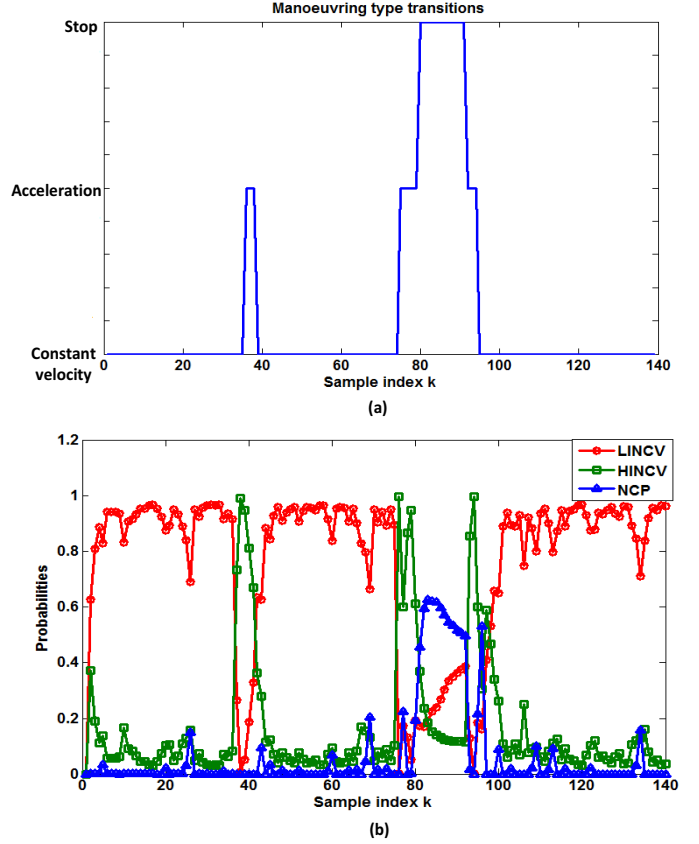


Fig. 4. The movement mode transition and model probabilities: (a) the actual manoeuvring type (b) the estimated model probabilities by the proposed method (with the particle number being 2500 for each model,  $P_d=0.8$  and  $\sigma_r=1.0$ ).

for the NRDB-MM was set exactly the same as in [12]. For the two particle-filtering-based methods, i.e. the proposed method and the MMPF, the number of particles corresponding to each state model (denoted as  $N$ ) was chosen at different levels so that we can assess its impact on the accuracy of the estimation.

For each approach, 100 Monte-Carlo simulation experiments were carried out and the root mean square estimation errors (RMSEs) averaged over the 100 simulations at different time instances were calculated. We first focus on the average RMSE obtained by the different methods, as displayed in Figure 5. It can be seen from Figure 5 that:

(i) The proposed method achieved the best performance with the smallest errors during the most of the time instances than its counterparts, especially for the sample indexes between 80–92 when the target stopped.

(ii) Compared with the MMPF approach, the proposed method was less sensitive to the number of particles. Figure 5 shows that the errors for the MMPF method were substantially increased when the number of particles reduced from  $N = 2500$  to  $N = 1000$ . In contrast, similar performances were obtained for the proposed method with different particle sizes.

There are several reasons for these differences. First, in comparison with the NRDB-MM algorithm, the proposed approach adopts the particle-filtering-based method, and therefore it avoids the approximations made in the GMM-based NRDB approach in [12], leading to a performance improvement over the NRDB-MM algorithm. Secondly, compared the MMPF approach, a novel sampling method is proposed to incorporate either the measurement information (when measurements are recorded) or knowledge on the Doppler blindness constraint (when no measurements are recorded) for the construction of the

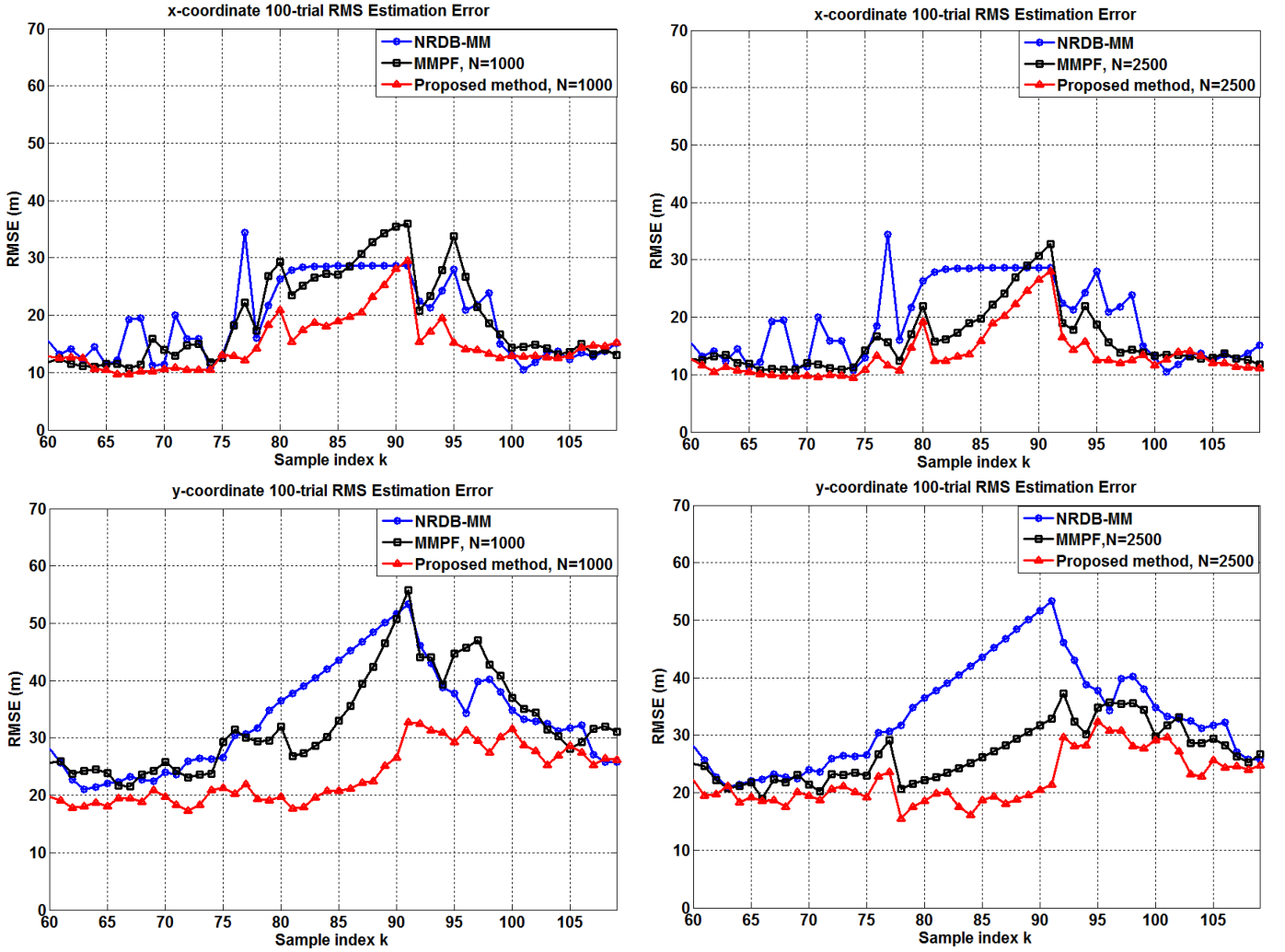


Fig. 5. The RMSEs averaged over 100 simulation experiments for different approaches (with  $P_d=0.8$  and  $\sigma_r=1.0$ ).

importance distributions. Effective particles can thus be sampled from the constructed importance distributions, which leads to a more accurate state estimation even with a relatively small particle size.

Finally, we focus on vehicle tracking when the vehicle was standstill and hence was within the Doppler blindness constraint region. This is a challenging scenario because no measurements was recorded during the vehicle stopping interval. For this end, we considered the same parameter settings as did in [12], including different detection probabilities  $P_D$  and the standard deviations of range rate measurement  $\sigma_r$ . A comprehensive evaluation was performed under these parameter settings to compare different approaches.

Under each parameter setting, the RMSEs during the time interval when the vehicle stopped for different approaches were calculated. Tables I and II display the average RMSEs over the 100 simulation experiments. It can be seen from the two tables that the proposed approach outperformed the other methods with the smallest tracking errors. This shows that for the scenario where the vehicle stopped and no measurements were recorded, the proposed approach could most efficiently utilize knowledge on the Doppler blindness constraint for vehicle tracking.

### C. Computational costs

In this subsection, we briefly evaluate the computational cost of different methods. The execution was performed on a PC with 3.40

GHz processing speed and 8.00 GB memory using Matlab 2013(a). For the scenario under investigation, the vehicle moved 700 seconds and the measurement was taken every 5 seconds, so it was required that the computation time for processing one sample was less than 5s. In total there were  $700/5=140$  sample time indexes (time steps).

For each method considered in the simulation study, the execution time and the average processing time for each sample were recorded, as displayed in Table III. We can see that the computational costs of all the algorithms for processing one sample are far less than 5s and fast enough to make the tracking algorithm run in practice. Further reduction of the computation time can be achieved by implementing the algorithm in C/C++ programming environment.

## V. CONCLUSIONS

In this paper, a novel particle filtering approach for GMTI tracking has been developed. The proposed particle filter makes use of the EKF and its generalized version in [12] to construct importance distributions for efficient generation of particles. In comparison with the GMM-based NRDB algorithm recently developed in [12], the three approximations outlined in the introduction section can be satisfactorily addressed by the proposed algorithm, so that more accurate state filtering can be obtained. On the other hand, comparing to general-purpose particle filters, where the importance distribution is usually chosen as the state transition distribution, the information

TABLE I  
THE RMSES (m) AVERAGED OVER 100 EXPERIMENTS IN X-COORDINATE WITHOUT RECORDED MEASUREMENTS.

| Scenario                  | I     | II    | III   | IV    | V     | VI    | VII   | VIII  |
|---------------------------|-------|-------|-------|-------|-------|-------|-------|-------|
| $P_d$                     | 0.6   | 0.6   | 0.6   | 0.6   | 0.8   | 0.8   | 0.8   | 0.8   |
| $\sigma_{\dot{r}}$ (m/s)  | 1.5   | 1.0   | 0.75  | 0.6   | 1.5   | 1.0   | 0.75  | 0.6   |
| $\kappa/\sigma_{\dot{r}}$ | 2     | 3     | 4     | 5     | 2     | 3     | 4     | 5     |
| NRDB-MM [12]              | 55.52 | 51.37 | 57.48 | 50.57 | 28.51 | 29.60 | 26.45 | 27.51 |
| MMPF (N=1000)             | 51.04 | 52.50 | 55.20 | 48.51 | 37.15 | 29.21 | 29.77 | 28.76 |
| MMPF (N=2500)             | 46.30 | 37.75 | 46.41 | 37.61 | 27.59 | 26.11 | 27.87 | 27.92 |
| Proposed method (N=1000)  | 28.23 | 29.41 | 29.75 | 30.42 | 24.74 | 22.47 | 27.98 | 22.16 |
| Proposed method (N=2500)  | 26.89 | 30.40 | 29.32 | 29.46 | 22.02 | 20.01 | 26.14 | 21.45 |

TABLE II  
THE RMSES (m) AVERAGED OVER 100 EXPERIMENTS IN Y-COORDINATE WITHOUT RECORDED MEASUREMENTS.

| Scenario                  | I     | II    | III   | IV    | V     | VI    | VII   | VIII  |
|---------------------------|-------|-------|-------|-------|-------|-------|-------|-------|
| $P_d$                     | 0.6   | 0.6   | 0.6   | 0.6   | 0.8   | 0.8   | 0.8   | 0.8   |
| $\sigma_{\dot{r}}$ (m/s)  | 1.5   | 1.0   | 0.75  | 0.6   | 1.5   | 1.0   | 0.75  | 0.6   |
| $\kappa/\sigma_{\dot{r}}$ | 2     | 3     | 4     | 5     | 2     | 3     | 4     | 5     |
| NRDB-MM [12]              | 43.55 | 56.95 | 56.81 | 53.99 | 37.57 | 44.69 | 58.73 | 51.86 |
| MMPF (N=1000)             | 51.56 | 55.85 | 55.43 | 52.57 | 43.86 | 39.01 | 47.59 | 53.16 |
| MMPF (N=2500)             | 33.29 | 50.06 | 42.33 | 46.56 | 35.75 | 26.18 | 41.94 | 44.23 |
| Proposed method (N=1000)  | 28.61 | 30.41 | 30.59 | 33.43 | 28.45 | 22.85 | 28.46 | 32.02 |
| Proposed method (N=2500)  | 26.32 | 24.82 | 25.93 | 29.86 | 25.74 | 20.59 | 23.43 | 30.68 |

TABLE III  
THE COMPUTATIONAL COSTS FOR DIFFERENT APPROACHES

|  | NRDB-MM | MMPF (N=1000) | MMPF (N=2500) | Proposed method (N=1000) | Proposed method (N=2500) |
|--|---------|---------------|---------------|--------------------------|--------------------------|
| Total execution time (s)                     | 3.28    | 0.90          | 4.18          | 1.51                     | 4.47                     |
| Execution time for one sample ( $10^{-2}$ s) | 2.34    | 0.64          | 2.99          | 1.08                     | 3.19                     |

on both the measurements and the Doppler blindness constraint can be directly incorporated in the proposed method when forming the importance distributions. As a result, it has substantially enhanced the quality of the particle filter. The numerical results in the Monte Carlo simulation has verified that the proposed method outperformed the existing methods with an acceptable computational cost.

## REFERENCES

- [1] Whitaker, J. *The Electronics Handbook, Second Edition*, Taylor Francis Group: CRC Press, 2005.
- [2] Mertens, M., and Ulmke, M. "Precision GMTI tracking using road constraints with visibility information and a refined sensor model," in *2008 IEEE Radar Conference, Rome, Italy*, 2008.
- [3] Kirubarajan, T., Bar-Shalom, Y., Pattipati, K., and Kadar, I. "Ground target tracking with topography-based variable structure IMM estimator," *Aerospace and Electronic Systems, IEEE Transactions on*, vol. 36, no. 1, pp. 26–46, 2000.
- [4] Arulampalam, M., Gordon, N., Orton, M., and Ristic, B. "A variable structure multiple model particle filter for GMTI tracking," in *Proc. of the Fifth International Conference on Information Fusion, Annapolis, MD, USA*, 2002.
- [5] Payne, O., Gordon, N., and Marrs, A. "An unscented particle filter for GMTI tracking," in *2004 IEEE Aerospace Conference, Big Sky, Montana, USA*, 2004.
- [6] Merve, R., Doucet, A., Freitas, N., and Wan, E. "The unscented particle filter," *Technical Report, Cambridge University Engineering Department*, 2000.
- [7] Kirubarajan, T., and Bar-Shalom, Y. "Tracking evasive move-stop-move targets with a GMTI radar using a VS-IMM estimator," *Aerospace and Electronic Systems, IEEE Transactions on*, vol. 39, no. 3, pp. 1098–1103, July 2003.
- [8] Koch, W. "On exploiting 'negative' sensor evidence for target tracking and sensor data fusion," *Information Fusion*, vol. 8, no. 1, pp. 28–39, 2007.
- [9] Ulmke, M., Eedinc, O., and Willett, P. "GMTI tracking via the Gaussian mixture cardinalized probability hypothesis density filter," *Aerospace and Electronic Systems, IEEE Transactions on*, vol. 46, no. 4, pp. 1821–1833, 2010.
- [10] Musicki, D., and Hanselmann, T. "State dependent detection and object tracking," in *Proc. of the IEEE International Conference on Multisensor Fusion and Integration for Intelligent Systems, Seoul, Korea*, 2008.
- [11] Agate, C., Wilkerson, R., and Sullivan, K. "Utilizing negative information to track ground vehicles through move-stop-move cycles," in *Proc. of Signal Processing, Sensor Fusion, and Target Recognition XIII, SPIE, Orlando, FL, USA*, 2004.
- [12] Clark, J., Kountouriotis, P., and Vinter, R. "A new Gaussian mixture algorithm for GMTI tracking under a minimum detectable velocity constraint," *Automatic Control, IEEE Transactions on*, vol. 54, no. 12, pp. 2745–2756, December 2009.
- [13] Salmond, D. "Mixture reduction algorithms for target tracking in clutter," in *Proc. of SPIE Signal Data Processing of Small Targets, Los Angeles, CA, USA*, 1990.
- [14] Curry, R. *Estimation and Control With Quantized Measurements*, Cambridge, MA: MIT Press, 1970.
- [15] Blom, H., and Bloem, E. "Exact Bayesian and particle filtering of stochastic hybrid systems," *Aerospace and Electronic Systems, IEEE Transactions on*, vol. 43, no. 1, pp. 55–70, 2007.
- [16] Ristic, B., Arulampalam, S., and Gordon, N. *Beyond the Kalman filter Particle filters for tracking applications*, Norwood, MA: Artech House, 2004.
- [17] Longbin, M., Song, X., Zhou, Y., Sun, Z., and Bar-Shalom, Y. "Un-biased converted measurements for tracking," *Aerospace and Electronic Systems, IEEE Transactions on*, vol. 34, no. 3, pp. 1023–1027, 1998.
- [18] Mallick, M., and Arulampalam, S. "Comparison of nonlinear filtering algorithms in ground moving target indicator (GMTI) tracking," in *Proc. Signal and Data Processing of Small Targets, San Diego, CA*, 2003.
- [19] Bar-Shalom, Y., Willett, P., and Tian, X. *Tracking and Data Fusion: A Handbook of Algorithms*, YBS Publishing, 2011.
- [20] Haug, A. *Bayesian Estimation and Tracking: A Practical Guide*, New York, Wiley, 2012.
- [21] Li, X., and Jilkov, P. "Survey of maneuvering target tracking, part I: Dynamic models," *Aerospace and Electronic Systems, IEEE Transactions on*, vol. 39, no. 4, pp. 1333–1364, 2003.
- [22] Kelly, D., and Boland, F. "Motion model selection in tracking humans," in *IET Irish Signals and Systems Conference, Dublin, Ireland*, 2006.
- [23] Zhang, S., and Bar-Shalom, Y. "Tracking move-stop-move targets with state-dependent mode transition probabilities," *Aerospace and Electronic Systems, IEEE Transactions on*, vol. 47, no. 3, pp. 2037–2054, 2011.



- [24] Mallick, M., and La Scala, B. "Comparison of single-point and two-point difference track initiation algorithms using position measurements," in *International Colloquium on Information Fusion, Xi'an, China, 2007*.
- [25] Yeom, S., Kirubarajan, T., and Bar-Shalom, Y. "Track segment association, fine-step IMM and initialization with doppler for improved track performance," *Aerospace and Electronic Systems, IEEE Transactions on*, vol. 40, no. 1, pp. 293–309, 2004.
- [26] Koutsoukos, X., James, K., and Feng, Z. "Monitoring and diagnosis of hybrid systems using particle filtering methods," in *Proc. of the Fifteenth International Symposium on the Mathematical Theory of Networks and Systems (MTNS'02), Notre Dame, IN, USA, 2002*.

## APPENDIX

### A. Mean and variance conditional on an interval-censored measurement

We summarise the results on the mathematical expectation and variance conditional on some interval-censored measurements below; see [14] for details.

Consider a measurement  $m$  given by  $m = \mathbf{q}^T \mathbf{x} + w$  with  $w \sim \mathcal{N}(w|0, \sigma^2)$ . Assume that the prior distribution of the state vector  $\mathbf{x}$  is Gaussian,  $\mathcal{N}(\mathbf{x}|\hat{\mathbf{x}}_0, \mathbf{P}_0)$ . Let  $A$  denote an interval  $A = [a, b]$ .

Let  $\mu = \mathbf{q}^T \hat{\mathbf{x}}_0$ . Given that  $m$  falls into  $A$ , the conditional expectation and covariance are:

$$E(\mathbf{x}|m \in A) = \hat{\mathbf{x}}_0 + \mathbf{K}[\hat{m}_A - \mu], \quad (36)$$

$$\text{cov}(\mathbf{x}|m \in A) = \mathbf{P} + \mathbf{K}\mathbf{V}_A\mathbf{K}^T, \quad (37)$$

where

$$\mathbf{K} = \mathbf{P}_0\mathbf{q}(\mathbf{q}^T\mathbf{P}_0\mathbf{q} + \sigma^2)^{-1}, \quad (38)$$

$$\mathbf{P} = \mathbf{P}_0 - \mathbf{K}\mathbf{q}^T\mathbf{P}_0, \quad (39)$$

$$\hat{m}_A = E[m|m \in A] = c^{-1}\bar{\sigma}^2[\mathcal{N}(a|\mu, \bar{\sigma}^2) - \mathcal{N}(b|\mu, \bar{\sigma}^2)] + \mu, \quad (40)$$

$$\begin{aligned} \mathbf{V}_A &= \text{cov}[m|m \in A] \\ &= c^{-1}\bar{\sigma}^2[(a + \mu)\mathcal{N}(a|\mu, \bar{\sigma}^2) \\ &\quad - (b + \mu)\mathcal{N}(b|\mu, \bar{\sigma}^2)] + (\mu^2 + \bar{\sigma}^2) - \hat{m}_A^2. \end{aligned} \quad (41)$$

The parameter  $\bar{\sigma}^2$  is estimated as  $\bar{\sigma}^2 = \mathbf{q}^T\mathbf{P}_0\mathbf{q} + \sigma^2$ , and  $c$  in (41) is a normalizing constant ensuring that the corresponding probability density integrates to unity, i.e.  $c = \int_a^b \mathcal{N}(m|\mu, \bar{\sigma}^2)dm$ .

### B. Rank-deficient process noise

In many practical problems, the state transition probability distribution given by the state equation is rank-deficient (see, e.g. [21]). Consider the following state transition equation:

$$\mathbf{x}_t = \mathbf{F}(m_t)\mathbf{x}_{t-1} + \mathbf{G}_t\mathbf{w}_{t-1}(m_t) \quad (42)$$

where  $\mathbf{x}_t$  is an  $n$ -dimensional state vector.  $\mathbf{G}_t$  is an  $n \times q$  matrix with  $n > q$  and  $\mathbf{w}_{t-1}(m_t) \in R^q$ . In this case,  $\mathbf{x}_t$  is constrained in a vector space with the deficient rank  $q < n$ . As a consequence, if particles  $\mathbf{x}_t^i$  are sampled from an importance distribution in  $R^n$ , they may fall outside the required vector space and the corresponding state transition probability then could not be calculated. Clearly, an accept-reject method where samples  $\mathbf{x}_t^i$  outside the given space are discarded is very inefficient.

In order to solve this rank-deficient problem, we perform the QR decomposition for the matrix  $\mathbf{G}_t$  as:

$$\mathbf{G}_t = \mathbf{U}_t\mathbf{W}_t, \quad (43)$$

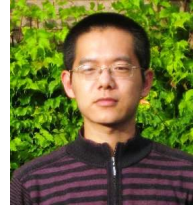
where  $\mathbf{W}_t = [\Lambda_t, \mathbf{0}]^T$ .  $\Lambda_t$  is a matrix with rank  $q$  and  $\mathbf{U}_t$  is an orthogonal matrix. We define:

$$\mathbf{s}_t = \begin{bmatrix} \mathbf{s}_{1,t} \\ \mathbf{s}_{2,t} \end{bmatrix} = \mathbf{U}_t^T \mathbf{x}_t, \quad (44)$$

and let  $\mathbf{U}_t^T = [\mathbf{U}_{1,t}, \mathbf{U}_{2,t}]^T$ ,  $\tilde{f}_1(\mathbf{x}_{t-1}, m_t) = \mathbf{U}_{1,t}^T F(m_t)\mathbf{x}_{t-1}$  and  $\tilde{f}_2(\mathbf{x}_{t-1}, m_t) = \mathbf{U}_{2,t}^T F(m_t)\mathbf{x}_{t-1}$ . Eq. (42) then becomes:

$$\begin{bmatrix} \mathbf{s}_{1,t} \\ \mathbf{s}_{2,t} \end{bmatrix} = \begin{bmatrix} \tilde{f}_1(\mathbf{x}_{t-1}, m_t) + \Lambda_t^T \mathbf{w}_{t-1} \\ \tilde{f}_2(\mathbf{x}_{t-1}, m_t) \end{bmatrix}. \quad (45)$$

From Eq. (45), we can see that by transforming  $\mathbf{x}_t$  to  $\mathbf{s}_t$ , the state transition function is split into a stochastic part  $\mathbf{s}_{1,t}$  and a deterministic part  $\mathbf{s}_{2,t}$ . The deterministic part  $\mathbf{s}_{2,t}$  can be directly worked out from the previous state value. Therefore, we apply the developed method only to generate particles that are related to the stochastic part  $\mathbf{s}_{1,t}$ . The obtained particles for  $\mathbf{s}_{1,t}$  and  $\mathbf{s}_{2,t}$  are then transformed back to the original scale.



**Dr. Miao Yu** (M15) was born in China in 1986. He obtained his MSc degree in digital communication system and PhD degree in the applications of computer vision based techniques for fall detection, in the Department of Electronic and Electrical Engineering, Loughborough University, U.K, in 2008 and 2013 respectively. From 2013 until now, he works as a research associate in the Department of Aeronautical and Automotive Engineering, Loughborough University. Currently his major research area focuses on the application of the domain knowledge in improving the signal processing performance, especially for the object tracking.



**Dr. Cunjia Liu** received his B.Eng. and M.Sc. degrees in guidance, navigation, and control from Beihang University, Beijing, China, in 2005 and 2008, respectively. In 2011, he received a Ph.D. degree in autonomous vehicle control from Loughborough University, Loughborough, U.K. From 2011, he was a Research Associate with the Department of Aeronautical and Automotive Engineering at Loughborough University, where he was appointed as a Lecturer in flight dynamics and control in 2013. His current research interests include optimization-based control, disturbance-observer-based control, Bayesian information fusion and their applications to autonomous vehicles for flight control, path planning, decision making, and situation awareness.



**Prof. Baibing Li** received a B.Sc. degree from Yunnan University, Kunming, China, an M.Sc. degree from Shanghai Jiao Tong University, Shanghai, China, and an M.Sc. degree from Vrije Universiteit Brussel, Brussels, Belgium. In 1991, he received a Ph.D. degree from the Management School, Shanghai Jiao Tong University. He was a Postdoctoral Research Fellow with Katholieke Universiteit Leuven, Leuven, Belgium, and a Research Associate with Newcastle University, Newcastle upon Tyne, UK. In 2001, he was appointed as a Lecturer at Newcastle University. In 2004, he moved to the School of Business and Economics, Loughborough University, Loughborough, UK, as a Lecturer, where he was subsequently appointed as a Reader in 2007 and a Professor in 2011. His current research interests cover Bayesian statistical modelling and forecasting for Gaussian and non-Gaussian dynamic problems in various management areas. In recent years, much of his work has also involved transport and traffic management such as transportation demand analysis, travel behaviour modelling, and intelligent transportation systems.

He is a member of IEEE and a member of the Royal Statistical Society.



**Prof. Wen-Hua Chen** (M'00-SM'06) received the M.Sc. and Ph.D. degrees from Northeast University, Shenyang China, in 1989 and 1991, respectively. From 1991 to 1996, he was a Lecturer and then Associate Professor with the Department of Automatic Control, Nanjing University of Aeronautics and Astronautics, Nanjing, China. From 1997 to 2000, he held a research position and then a Lecturer in control engineering with the Centre for Systems and Control, University of Glasgow, Glasgow, UK.

In 2000, he moved to the Department of Aeronautical and Automotive Engineering, Loughborough University, Loughborough, UK, as a Lecturer, where he was appointed as a Professor in 2012. His research interests include the development of advanced control strategies (Nonlinear Model Predictive Control, Disturbance Observer Based Control, etc.) and their applications in aerospace and automotive engineering. Currently, much of his work has also involved in the development of Unmanned Autonomous Intelligent Systems.

He is a Fellow of the Institution of Engineering and Technology and Institution of Mechanical Engineers and a Senior Member of IEEE.

#### Figures:

Fig. 1. The speed of the manoeuvring ground vehicle.

Fig. 2. The trajectories of the ground target and sensor platform.

Fig. 3. The target radial velocities. When the vehicle stops (the target radial velocities are zero), no measurements are recorded.

Fig. 4. The movement mode transition and model probabilities: (a) the actual manoeuvring type (b) the estimated model probabilities by the proposed method (with the particle number being 2500 for each model,  $P_d=0.8$  and  $\sigma_r=1.0$ ).

Fig. 5. The RMSEs averaged over 100 simulation experiments for different approaches (with  $P_d=0.8$  and  $\sigma_r=1.0$ ).